doi:10.1038/nature09601

1. Description of the EDGES radio spectrometer

Determining the evolution of the mean redshifted 21-cm brightness temperature during reionization and the Dark Ages requires a low-frequency radio spectrometer to measure the all sky spectrum below 200 MHz. Interferometers are not suited to this application since they lack effective zero-baseline measurements. The sky spectrum at these frequencies ranges from 100 to 10,000 K, depending on position and frequency, and follows an extremely smooth, nearly power-law spectrum[2,10] given by $T \propto \nu^{-2.5}$. Galactic synchrotron emission is the dominate component of the astrophysical emission accounting for ~70%, with free-free emission and discrete Galactic and extragalactic continuum sources contributing the remainder[14]. Radio recombination lines (RRLs) in the interstellar medium are an exception to the smooth spectrum, but they are extremely faint and occur at discrete, known frequencies, that can be excised in observations. In contrast, the mean redshifted 21-cm contribution is ~10 mK and is predicted to follow a fiducial spectral shape[13], exhibiting potentially rapid changes at several milestones in the history of the IGM, including during reionization.

Isolating the 21-cm signal from the Galactic and extragalactic emission imposes two high-precision requirements on the spectrometer. First, instrumental artifacts and systematic errors must be eliminated to below 1 mK (*rms*) so that they are sub-dominate to the 21-cm signal for optimal data analysis. Second, separation of the foreground spectrum, either by subtraction of a highly-accurate model or empirical fit, must be achieved at better than 1 part in 10^4. The usual solution in radio astronomy to the first requirement is to use a blank reference field to precisely calibrate the instrumental response. This is not possible for all-sky global 21-cm measurements.

The approach we have followed is to implement a high dynamic-range, high linearity spectrometer using an internal comparison source between the antenna and spectrometer receiver for instrumental calibration. An internal comparison source necessitates special care in the system to ensure that the propagation of the sky signal through the antenna into the receiver is well controlled and understood since its path is not calibrated by the internal comparison. In addition, the common presence of strong, variable RFI at most radio observing sites dictates additional linearity and sampling stability in the analog-to-digital conversion.

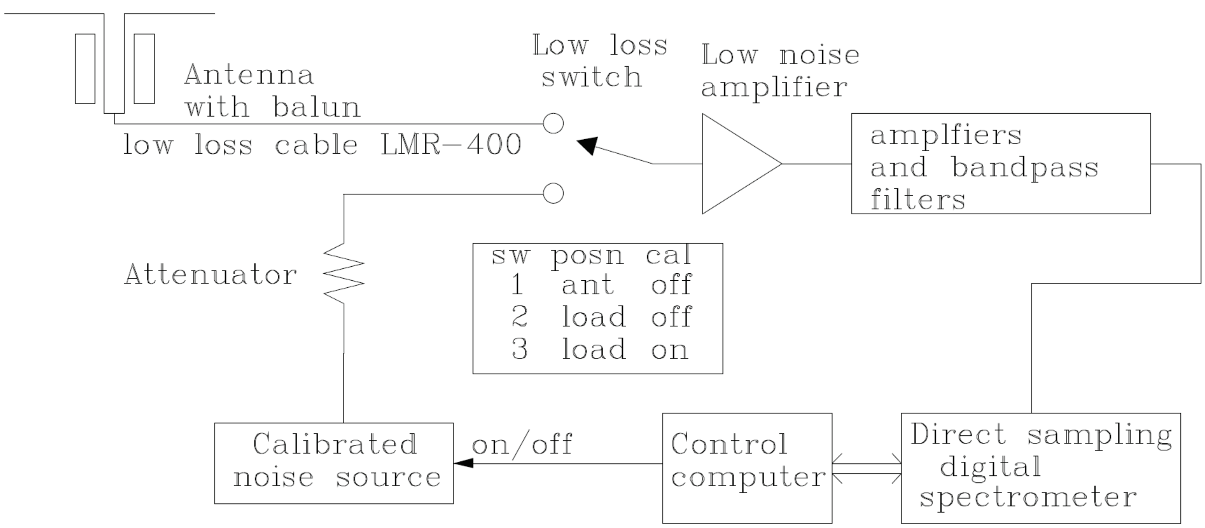

Figure S1. *Block schematic of the EDGES internal-comparison spectrometer.*

The EDGES system consisted of three modules as illustrated in Figures S1 and S2: an antenna, an amplifier and comparison switching module, and a digital backend for analog-to-digital conversion and storage. The antenna was a modified dipole and was compact and planar in order to reduce self-reflections and placed over a conducting mesh resting directly on the ground in order to eliminate reflections from the ground and to reduce gain toward the horizon. The amplifier module was connected directly to the antenna (through a ferrite core balun) without transmission cables to reduce the impact of reflections due to impedance mismatch within the electrical path of the instrument. The amplifier chain was connected through a voltage controlled switch to one of three inputs: the antenna, an ambient load, or an ambient load plus a calibration noise source. Switching between the ambient load and the antenna provides the comparison to subtract instrumental artifacts from the measured sky spectrum. The digital backend was an off-the-self digitizer contained on a PCI card connected to a host computer.

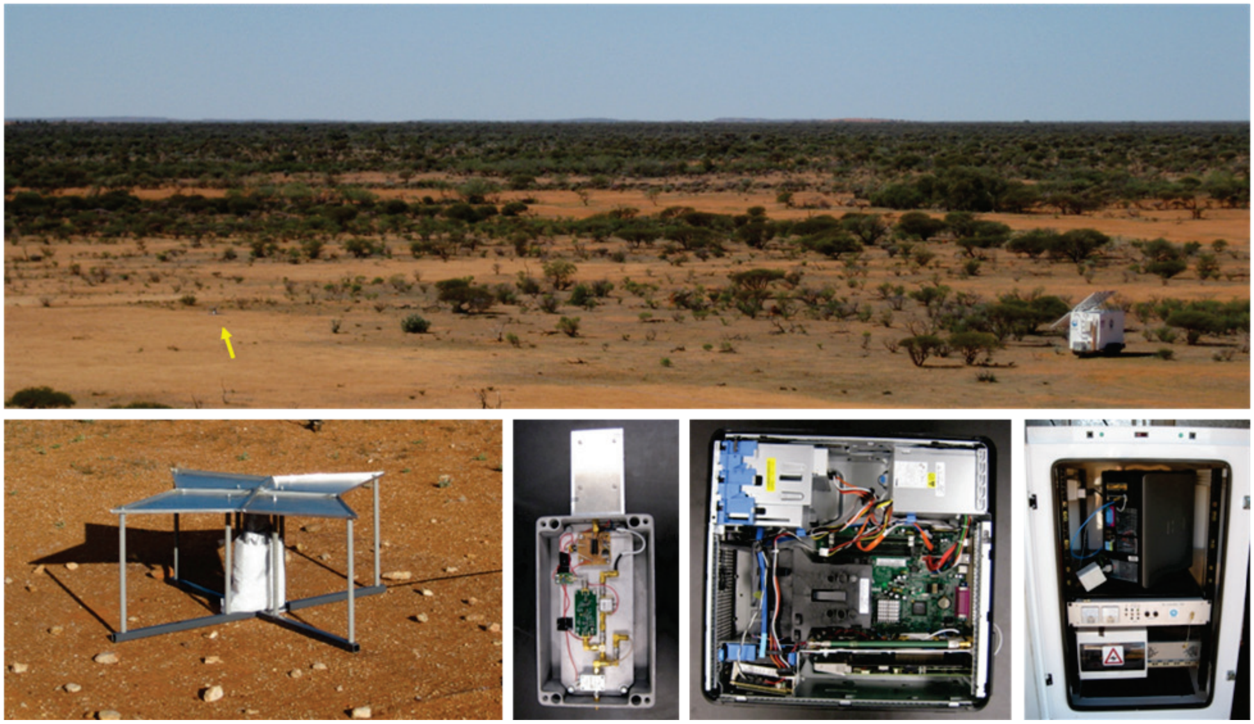

Figure S2. *EDGES instrument deployed at the Murchison Radio-astronomy Observatory in Western Australia in September, 2009. The top panel shows the full experiment, with the location of the antenna indicated by the yellow arrow. The bottom panels show, from left to right, the four-point dipole antenna; comparison-switched receiver; data acquisition computer with internal custom analog filtering and control boards; and arrangement of components in a Faraday enclosure inside the CSIRO support trailer.*

1.1. Analog-to-Digital Conversion

Preliminary investigations demonstrated that the digital backend is a critical component for achieving the high dynamic-range requirements of the ultra-clean spectrometer. For the deployment reported here, EDGES used a commercial Agilent U1070A / Acqiris DP310 12-bit, 420 MS/s, high-speed PCI digitizer. This board has good performance in the following areas: sample clock timing stability (low jitter), spurious free dynamic range, low total harmonic distortion (high linearity) and analog-digital isolation. Raw 12-bit samples were transferred from the Agilent board via the PCI bus within the host PC and the spectrum was computed on by the CPU by performing a fast Fourier Transform (FFT) using a Blackman-Harris window function to improve channel isolation. The integration efficiency was approximately 10%.

Full simulations with this digital backend showed that systematics resulting from digitizer non-linearity in the presence of strong RFI from Orbcomm low earth orbit satellites (a primary source of RFI at radio-quiet sites in the target frequencies) would be under < 6 mK (EDGES Memo #41, http://www.haystack.mit.edu/ast/arrays/Edges). Characterization of the receiver was performed in the laboratory by observing filtered broadband noise designed to produce a spectrum close to that expected from the antenna looking at the sky. Strong continuous-wave signals were added to simulate the RFI environment. In astronomical operation, we reached a thermal uncertainty limit of ~30 mK per native 13 kHz spectral channel with no indication of systematic contributions from the digitizer. Binning the integrated spectrum to lower spectral resolution of 1 MHz reached an *rms* limit of ~10 mK. Analysis of the integrated spectrum suggested that faint, un-excised RFI at approximately the level of the thermal noise appeared to be a greater contribution than internal digitizer effects to non-thermal noise in the final measurement.

1.2. Compact, Planar, Dual-Octave Antenna and Ground Screen

A broadband, well-matched antenna with little frequency-dependent behavior reduces reflections within the RF path and minimizes the effects of a changing beam-pattern that act to mix angular structure in the sky to spectral structure in the measurement. We adapted the "four-point" antenna of Suh[15,16] to achieve the desired properties. This planar antenna design was utilized for EDGES to reduce the risk of reflections within the antenna itself. The size of the antenna was restricted to less than a wavelength (approximately 1.5 m) at the highest target frequency to ensure that any spectral ripples produced by internal reflections have a period much longer than the frequency extent expected for the 21-cm signatures. The EDGES antenna was matched well to the impedance of the first-stage amplifier between 130 and 190 MHz, with a reflection coefficient better than -10 dB over that band. A small corresponding ground screen was also included with the antenna to reduce loss while also limiting complications to the antenna power response profile from the shape and size of the screen itself. The relatively simple structure facilitated modeling with EM software.

2. Calibration and Data Interpretation

The internal comparison-switched calibration scheme was implemented in analog electronics using a low loss coaxial mechanical switch located immediately under the antenna that allowed the receiver input to be switched between two ports: 1) the antenna port, and 2) and internal port. The internal port was connected to an ambient temperature matched load, T_{load}, that was assumed to be consistent with the environmental temperature. An electronic switch was used to allow an additional calibrated noise source with *a priori* known temperature, T_{cal} (ν), to be coupled into the internal port in addition to the ambient load. The calibrated antenna spectrum, $T_{ant}(\nu)$, can be derived from this three-state switch cycle in units of absolute temperature referenced to the antenna input of the switch, according to:

(1) $$T_{ant}(\nu) = T_{cal}(\nu)\left[\frac{p_2(\nu)-p_0(\nu)}{p_1(\nu)-p_0(\nu)}\right] + T_{load}$$

where p_0, p_1, and p_2 are the power spectra from the three switch positions with contributions given as:

(2) $$\begin{aligned} p_0(\nu) &= g(\nu)\left[p_{load}(\nu) + p_{rcv}(\nu)\right] \\ p_1(\nu) &= g(\nu)\left[p_{cal}(\nu) + p_{load}(\nu) + p_{rcv}(\nu)\right] \\ p_2(\nu) &= g(\nu)\left[p_{ant}(\nu) + p_{rcv}(\nu)\right] \end{aligned}$$

Here, g is the collective gain of the amplifiers and bandpass filters in the analog receiver path, p_{load} is the noise power spectrum from the ambient temperature load, p_{rcv} is the noise spectrum from the first-stage low-noise amplifier (LNA) in the receiver, p_{cal} is the noise power spectrum from the calibrated noise source, and p_{ant} is the sky noise power spectrum after propagating through the antenna.

This calibration system effectively removes spurious signals produced by the digital electronics since they tend to be independent of the switch state and, hence, cancel out through the subtractions in Equation 1. And it removes the unknown constant gain contribution, g, through the divisions in Equation 1. It falls short, however, or calibrating the antenna transmission properties since the internal reference noise sources are located after the antenna in the electrical path. Any impedance mismatch between the antenna and receiver will produce a "calibrated" antenna spectrum, T_{ant}, that does not match the true sky spectrum. The relationship between the true sky spectrum and calibrated antenna spectrum produced by the EDGES internal calibration scheme is given by:

(3) $$T_{ant}(\nu) = \left[1-\left|\Gamma(\nu)\right|^2\right] T_{sky}(\nu) + \left[2\varepsilon\left|\Gamma\right|\cos(\beta) + \varepsilon^2\left|\Gamma\right|^2\cos^2(\beta) + (1-\varepsilon)^2\left|\Gamma\right|^2\right] T_{rcv}(\nu) \quad + \quad \cdots$$

where T_{sky} is the sky brightness convolved with the antenna beam, $|\Gamma|^2$ is the power reflection coefficient of the antenna due to its impedance mismatch with the 50 Ω input of the receiver, $T_{rcv,in}$ is the noise power that propagates out of the input to the first-stage LNA back toward the antenna, β is the phase shift due to the electrical path length between the receiver and antenna, and ε is the voltage correlation coefficient between the noise emitted at the input and output ports of the first-stage LNA. The first term in Equation 3 represents the power from the antenna that is directly propagated into the receiver. The second term of the equation is the receiver noise that is reflected from the the impedance mismatch at the boundary with the antenna and returns to the receiver. The sinusoidal terms are due to correlations between reflected receiver noise and receiver noise that propagates directly from the output of first-stage LNA into the rest of the receiver.

3. Selection of Observing Site

Strict requirements for the observing site were set based on calculations[9] of scattered receiver and Galactic noise, ionospheric and tropospheric scattering and propagation of RFI, and estimated lunar, aircraft, and meteor path losses for reflected RFI. For the measurements reported here, the instrument was deployed at the Murchison Radio-Astronomy Observatory in Western Australia. The support trailer was approximately 50 m from the antenna and the null of the dipole beam pattern was aligned toward the trailer. The horizon was free of obstructions above ~5 degrees. A low “breakaway” rock ridge partially surrounded the site at a distance of several hundred meters. Dry bushes and scrub were within several meters of the antenna. Very little RFI was detected outside of the satellite and aircraft bands, except following several periods of rain storms that created atmospheric conditions conducive to the propagation of signals from radio transmitters hundreds of km away. These conditions lasted several hours, typically, and occurred only about 5-10 times over three months.

REFERENCES

14. Bridle, A. H. The spectrum of the radio background between 13 and 404 MHz. Mon. Not. Roy. Astron. Soc.136, 219-240 (1967)

15. Suh, S. Y., Stutzman, W. L., and Davis, W. A. Low-profile, dual-polarized broadband antennas. *Ant. and Prop. Soc. Inter.Sym. IEEE*. 256–259 (2003)

16. Suh, S. Y., Stutzman, W., Davis, W., Waltho, A., Skeba, K., and Schiffer, J. A novel low-profile, dual-polarization, multi-band, base-station antenna element - the fourpoint antenna. *Vehic.Tech.Conf. IEEE.* 225–229 (2004)